**Title**
Metal Nanoparticles Catalyzed Selective Carbon-Carbon Bond Activation in the Liquid Phase.

**Authors**
Ye, Rong
Yuan, Bing
Zhao, Jie
et al.

Peer reviewed

# Metal Nanoparticles Catalyzed Selective Carbon−Carbon Bond Activation in the Liquid Phase

Rong Ye,[†,‡] Bing Yuan,[†] Jie Zhao,[†] Walter T. Ralston,[†] Chung-Yeh Wu,[†] Ebru Unel Barin,[†] F. Dean Toste,*[,†] and Gabor A. Somorjai*[,†,‡]

[†]Department of Chemistry, University of California, Berkeley, California 94720, United States
[‡]Chemical Science Division, Lawrence Berkeley National Laboratory, 1 Cyclotron Road, Berkeley, California 94720, United States

Ⓢ Supporting Information

**ABSTRACT:** Understanding the C−C bond activation mechanism is essential for developing the selective production of hydrocarbons in the petroleum industry and for selective polymer decomposition. In this work, ring-opening reactions of cyclopropane derivatives under hydrogen catalyzed by metal nanoparticles (NPs) in the liquid phase were studied. 40-atom rhodium (Rh) NPs, encapsulated by dendrimer molecules and supported in mesoporous silica, catalyzed the ring opening of cyclopropylbenzene at room temperature under hydrogen in benzene, and the turnover frequency (TOF)


Bond lengths were not drawn to scale.

was higher than other metals or the Rh homogeneous catalyst counterparts. Comparison of reactants with various substitution groups showed that electron donation on the three-membered ring boosted the TOF of ring opening. The linear products formed with 100% selectivity for ring opening of all reactants catalyzed by the Rh NP. Surface Rh(0) acted as the active site in the NP. The capping agent played an important role in the ring-opening reaction kinetics. Larger particle size tended to show higher TOF and smaller reaction activation energy for Rh NPs encapsulated in either dendrimer or poly(vinylpyrrolidone). The generation/size of dendrimer and surface group also affected the reaction rate and activation energy.
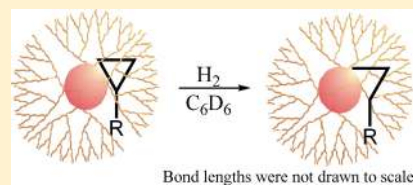
## 1. INTRODUCTION

Carbon−carbon (C−C) bond activation in the gas phase plays an important role in the chemical industry. Cracking and reforming reactions in crude oil refineries practice C−C bond activation on a large scale daily.[1] Polyethylene and polypropylene are currently the mostly widely used plastics, but their decomposition requires thermal C−C bond activation.[2] Due to thermodynamic and kinetic considerations, selective C−C bond activation is challenging.[3−6] Currently, these reactions are operated at high temperatures in industry (above 600 K). Undifferentiated thermal activation of C−C bond leads to multiple product formation simultaneously, requiring further product separation.

To overcome the low reactivity of C−C bonds, a practical strategy is to exploit the ring strain of (three- or four-membered) cyclic compounds as a driving force, thereby allowing the study of the factors controlling catalyst activity and selectivity. Early work[7,8] showed that catalytic cyclopropane hydrogenation (ring opening) by metal single crystal or powder catalysts in the gas phase was often accompanied by hydrogenolysis, forming smaller molecules. It was posited that the reaction mechanism was metal-dependent, proceeding through different intermediates including a monoadsorbed radical,[9] 1,3-diadsorbed species on Ni catalysts,[10] or metallocycle intermediate on Pt.[11]

In order to improve the product selectivity, efforts have been made to study C−C bond activation reactions using metal complexes of Rh,[12−16] Pt,[17] Pd,[18] Cu,[19] and other metals[20,21] in solution under relatively mild conditions. For example, Bart and Chirik[14] recently reported examples of ring opening of

cyclopropane derivatives catalyzed by organometallic Rh catalysts in the liquid phase and proposed the rhodium−metallocycle as the intermediate.

In this work, the advantages of both types of catalysis on the ring-opening reaction are combined: the high activity of heterogeneous catalysts and the high selectivity of homogeneous catalysts. We investigated the effect of different variables on the metal nanoparticles (NPs) catalyzed C−C bond activation in the liquid phase. Rh NPs catalyzed the ring opening of cyclopropylbenzene (**1**) at room temperature under an atmospheric pressure of H₂. The turnover frequency (TOF) of the reaction was correlated with reactant and metal NP properties, and the factors governing the catalytic activity and selectivity were analyzed.

## 2. RESULTS AND DISCUSSION

**2.1. Catalyst Screening.** The catalytic ring opening of **1** in the presence of H₂ was used as a model reaction to study the C−C bond activation reaction under mild conditions. The TOF of several potential catalysts for ring-opening reactions under atmospheric pressure of hydrogen in C₆D₆ was explored at 20 and 80 °C (Table 1). TOF of metal NPs was calculated by the number of molecules reacted in unit time (1 h) divided by the number of undercoordinated metal atoms, which was estimated from simple hard-sphere counting models.[22] 40-atom NPs of Rh, Pd, and Au encapsulated by fourth-generation polyamidoamine (PAMAM) dendrimer with hydroxyl terminal

**Table 1. Catalytic Ring Opening of Cyclopropylbenzene (1) with Various Catalysts Under 1 atm of $H_2$ in $C_6D_6$**

| entry | catalyst | TOF $(h^{-1})^a$ at 20 °C | TOF $(h^{-1})^a$ at 80 °C |
|---|---|---|---|
| 1 | $Rh_{40}$/G4OH/SBA-15 | 2.24 | 11.4 |
| 2 | $Pd_{40}$/G4OH/SBA-15 | 1.70 | 22.1 |
| 3 | $Au_{40}$/G4OH/SBA-15 | 0 | 0.20 |
| 4 | $(PPh_3)_3RhCl$ | 0.10 | $0.38^b$ |
| 5 | $[Rh(CO)_2Cl]_2$ | 0 | 0.10 |
| 6 | $Rh_{40}$/G4OH/SBA-15 + $PhICl_2$ | 0 | 0 |

$^a$Numbers of active sites for TOF calculation are estimated from simple hard-sphere counting models. $^b$This is the sum TOF for the formation of linear and branch products.

groups (G4OH) were synthesized and loaded into mesoporous silica SBA-15[23−26] (entries 1−3 in Table 1). Among these three catalysts, $Rh_{40}$/G4OH/SBA-15 offered the highest TOF at room temperature. Pd NPs were less active catalysts than Rh NPs at room temperature, but were more active at elevated temperature. The Au NPs showed very low activity as catalysts for this reaction. Rh(I) complexes such as the Wilkinson's catalyst $(PPh_3)_3RhCl$ and $[Rh(CO)_2Cl]_2$ had lower TOF compared to the Rh NPs. $(PPh_3)_3RhCl$ at 80 °C was the only case in Table 1 where the branch product cumene formed along with the linear product propylbenzene (branch:linear ratio about 1:2). Rh(III) compounds $RhCl_3$ or $Rh(acac)_3$ failed to catalyze the reaction. Oxidizing Rh in $Rh_{40}$/G4OH/SBA-15 by adding an organic oxidizer $PhICl_2$ completely inhibited the activity of the catalyst (entry 6 in Table 1). Pure mesoporous SBA-15 could not catalyze the reaction, which could be considered as the blank reaction. On the other hand, solid acids, such as $H^+$-Al-SBA-15 (acidified mesoporous silica SBA-15) and $H^+$-MFI (acidified mesoporous MFI zeolite), catalyzed the rearrangement of **1** to form only (E)-prop-1-en-1-ylbenzene at 80 °C without formation of propylbenzene, but they were inactive at room temperature. $Rh_{40}$/G4OH/SBA-15 also catalyzed the reaction in other solvents (toluene, dichloromethane, and methanol) with similar TOF to that in benzene.

**2.2. Characterization of $Rh_{40}$/G4OH/SBA-15.** TEM images of $Rh_{40}$/G4OH/SBA-15 before and after three cycles of reactions with **1** are shown in Figure 1A,B, respectively. The size of Rh NPs was 1.6 ± 0.2 nm by averaging over 100 particles. The NPs were stable after three cycles of reactions. No leaching was observed, as confirmed by the inductively coupled plasma optical emission spectrometry of the filtrate of the reaction mixture. Hydrogenolysis was not observable during the reaction, which was confirmed by the absence of small gas molecules in the headspace (the gas above the product solution) GC analysis. The mass balance (total amount of product and unreacted reactant after the reaction matched the amount of reactant before the reaction) provides additional support for the lack of hydrogenolysis. The rate of ring opening of **1** in the second and third cycle of the recycled catalyst was 97% and 96% of that in the first cycle, respectively. The as-synthesized $Rh_{40}$/G4OH/SBA-15 sample contained surface rhodium oxide species, according to the XPS spectrum (Figure 1C). The oxidation state of Rh after the reaction was purely 0, as shown by the 307.3 eV binding energy[24] in the XPS spectrum (Figure 1D). To explore the effects of these rhodium oxides on the kinetics of the ring-opening reaction, a set of control experiments with different pretreatment conditions were performed. Keeping all other variables the same, one
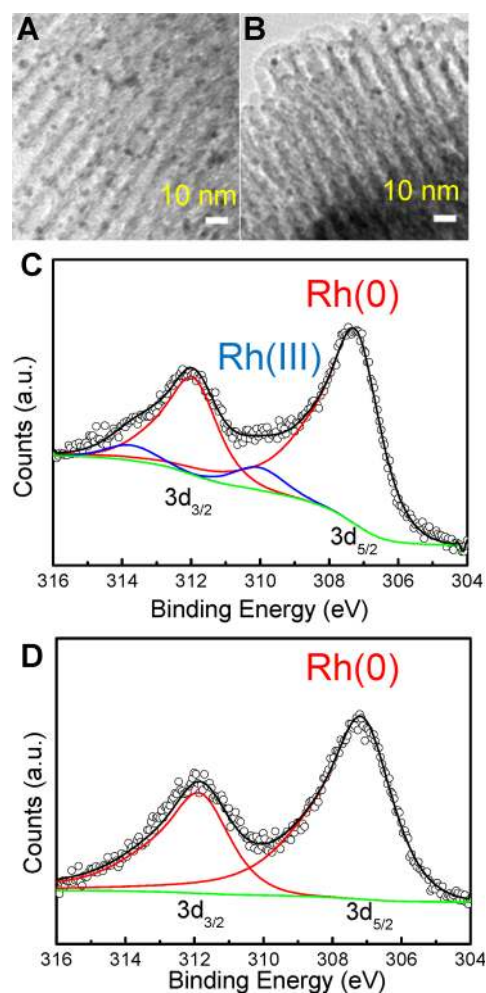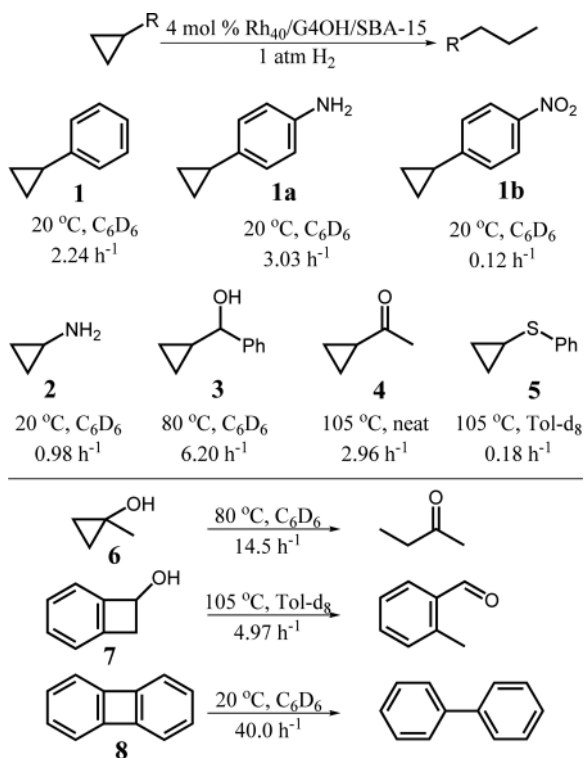


**Figure 1.** Characterization of $Rh_{40}$/G4OH/SBA-15. TEM images of the sample before (A) and after (B) three cycles of reactions. The scale bars are 10 nm. (C) and (D) Corresponding XPS spectra. XPS spectra are not normalized.

catalyst was mixed with $H_2$ at 100 °C for 24 h, one was mixed with Ar at 100 °C for 24 h, and the other without pretreatment. When these three catalysts were used in the reaction at 20 °C, they exhibited the same reaction rate/TOF on the ring opening of **1**. This implies that the reduction of the surface rhodium oxides to metallic rhodium was a fast process under reaction conditions.

**2.3. Applications on Other Cyclic Compounds.** Reactants that underwent the ring-opening reaction catalyzed by $Rh_{40}$/G4OH/SBA-15 are listed in Scheme 1 along with the TOF values under the specified conditions. Under the same reaction condition, the more electron-rich **1a** reacted faster than **1**, but reaction of electron-deficient **1b** was notably slower. It should be noted that a small amount of **1b** was reduced to **1a** during the reaction process, and the TOF reported for **1b** does not discount this pathway. Thus, the real TOF of **1b** ring-opening reaction is even smaller. The observation that ring opening was accelerated by electron-donating and decelerated by electron-withdrawing groups on the phenyl ring of the reactant is consistent with a hypothesis that a cationic intermediate is involved in the rate-limiting step of the reaction. This hypothesis held for molecules without phenyl rings. Rings attached to electron-donating groups opened quickly at a low temperature, while those attached to electron-withdrawing

**Scheme 1. Reactants for Ring-Opening Reactions Catalyzed by Rh$_{40}$/G4OH/SBA-15 and the TOF under Specified Reaction Condition**





**Figure 2.** Arrhenius plots of ring opening of **1** in $C_6D_6$ under $H_2$, catalyzed by Rh NPs of various sizes encapsulated in (A) G4OH and (B) PVP. (C) Plots of particle size and calculated ring-opening activation energy catalyzed by Rh NPs. The cartoons of dendrimer encapsulated NPs and PVP-capped NPs were shown in the bottom left and top right, respectively.

groups required higher temperatures to exhibit an observable reaction rate of C−C bond scission.

The TOF values in Scheme 1 were measured at various temperatures, which was a compromise of the low reaction rate at a low temperature and reactant/solvent boiling at a high temperature. Reactants **6** and **7**, rings attached to a hydroxyl group, underwent the ring-opening reaction with the hydroxyl group transformed to a carbonyl group. The formation of a C=O bond, which was not further hydrogenated under the reaction condition, provided an additional driving force for the ring-opening reaction. Thus, the TOF of **6** was high, and the typically inert four-membered ring in **7** was activated. In another example of four-membered ring C−C bond activation, biphenylene (**8**) was transformed to biphenyl at room temperature, a reaction for which homogeneous catalysts typically required elevated temperatures.[17]

The products from reactants **1**−**5** in Scheme 1 were entirely the linear/proximal ones. In contrast, Bart and Chirik[14] reported that the branch/distal products were favored by homogeneous Rh catalysts, unless a reactant with the ability to chelate with the Rh catalyst was used. The unique selectivity toward linear products by NPs in this work is likely attributed to a different reaction mechanism between the reported homogeneous catalysts and NP catalysts employed in this work.

**2.4. Kinetics Study of the Ring Opening Reaction of 1.** The size of dendrimer encapsulated NPs was tuned by modifying the Rh:G4OH ratio during the NP synthesis. Rh$_{15}$G4OH, Rh$_{40}$G4OH, and Rh$_{50}$G4OH were synthesized to explore the size effects of Rh NPs on the catalytic performance. However, synthesis of even larger sizes of G4OH-encapsulated NPs was limited to 4.5 nm in diameter by the size of G4OH. Figure 2A displays the temperature dependence of the ring opening TOF of **1** catalyzed by Rh NPs between 293 and 333
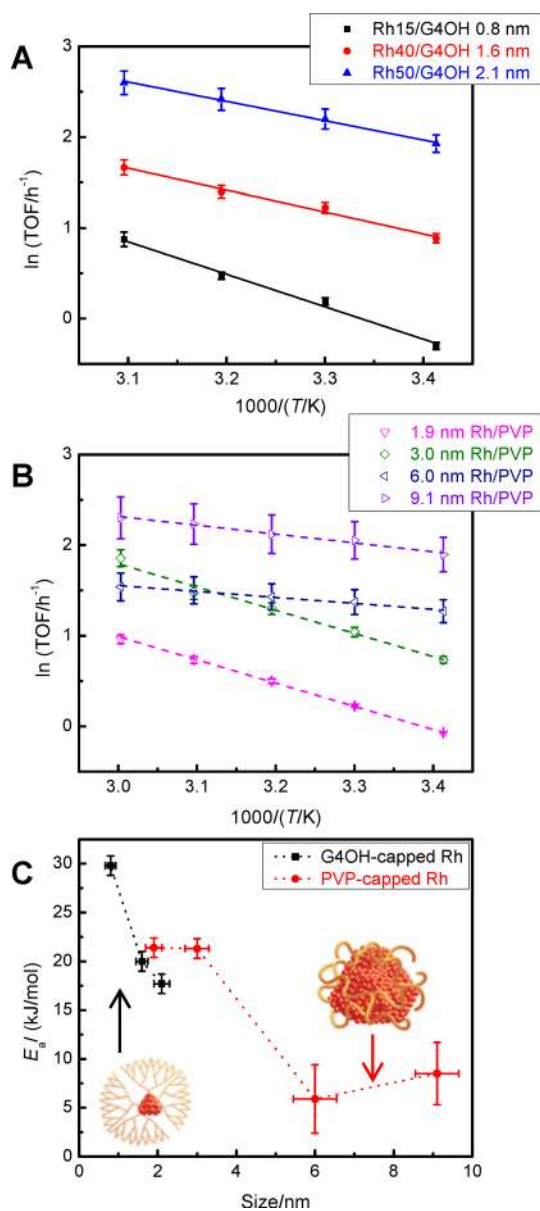
K in $C_6D_6$ under 1 atm of $H_2$. TOF increased as temperature increased for the same catalyst as expected. Further control experiments (data not reflected in the figure) with faster stirring rates gave the same TOF, suggesting that the reactions were not limited by diffusion under these reaction conditions. The apparent activation energy of ring opening catalyzed by each catalyst was determined from the slopes of the linear fit plots and plotted in Figure 2C. Keeping everything else constant, increasing the size of Rh NPs from 0.8 to 2.1 nm increased the TOF from 2.4 to 13.4 h$^{-1}$ (at 333 K) and decreased the reaction activation energy from 29.8 to 17.7 kJ/mol. The trend that larger particle size offered higher TOF has been previously observed in the catalytic hydrogenation of allyl alcohol[27] and alkynol[28] and dehydrogenation of ammonia borane.[29] The same size dependence of TOF and activation energy held for

the hydrogenation of styrene, an example of C−C $\pi$-bond hydrogenation (Figure S1).

On the basis of these observations, we hypothesized that the increased abundance of Rh−Rh bond on the surface of larger Rh NPs led to their higher catalytic activity. We tested the hypothesis with Rh NPs of various sizes encapsulated in polyvinylpyrrolidone (PVP). The Arrhenius plots of ring opening of **1** catalyzed by Rh/PVP NPs were shown in Figure 2B. The size effects of PVP capped NPs were the same as G4OH capped NPs. Here, the large Rh/PVP NPs (6.0 and 9.1 nm) had only a small percentage of undercoordinated surface atoms. With comparable amount of Rh loading, reactions catalyzed by large NPs had lower yield, due to scarcity of surface Rh atom, leading to a relatively large measurement error of TOF by NMR.

As shown in Figure 2C, comparing 2 nm Rh NPs capped by G4OH and PVP, the former had greater TOF. There were several possible reasons for this observation: (1) steric effect, the capping agent might block a portion of undercoordinated Rh atoms due to steric hindrance; (2) electronic effect, the interaction of the capping agent might tune the electronic structure of the Rh atoms, and thus affected the energetics of the reaction process.[30]

In order to elucidate the effects of the capping agent, Rh NPs encapsulated in different dendrimers were synthesized. Third-generation G3OH and sixth-generation G6OH were used in order to vary the size of the dendrimer without changing its chemical properties. The impact of the chemical properties of the dendrimer support was studied by replacing the terminal hydroxyl group in G4OH with primary amine and succinamic acid (SA) groups by using G4NH$_2$ and G4SA, respectively. Rh NPs were synthesized with these dendrimers, keeping the same amount of Rh and the Rh:dendrimer ratio as 40:1. TEM images of these Rh NPs indicated that the sizes were constant within error. Arrhenius plots of ring opening of **1** catalyzed by these NPs are given in Figure 3A, and the corresponding activation energy in Figure 3B. Modifying the dendrimer generation from G3OH to G6OH, the rate of ring opening tended to decrease and the corresponding activation energy generally increased, likely due to the steric effect. G4NH$_2$ and G4OH had similar size but distinct Lewis and Brønsted basicity, so the lower activity of Rh$_{40}$/G4NH$_2$ might result from an electronic effect. Both G4OH and G4SA have 64 surface groups, but −SA is much bulkier than −OH as shown in Figure 3B. Rh$_{40}$/G4SA showed smaller TOF than Rh$_{40}$/G4OH, mainly caused by the steric effects.

## 3. EXPERIMENTAL SECTION

**3.1. Chemicals.** Information about chemicals, including synthesis of supported NPs, organic reactants, and characterization methods, can be found in the Supporting Information.

**3.2. Representative Procedure for Catalytic Reactions.** To a dry 10 mL Schlenk flask, equipped with a stir bar, was added cyclopropylbenzene (8.9 mg, 0.075 mmol), Rh$_{40}$/G4OH/SBA-15 (50 mg, 0.003 mmol, 4 mol %), mesitylene (2.3 $\mu$L, internal standard, Aldrich), and benzene-$d_6$ (1 mL). The reaction mixture was degassed, placed under 1 atm of H$_2$, and heated with stirring at the desired temperature for 2 h. The mixture was then cooled to room temperature, and the solid catalyst filtered using a polytetrafluoroethylene syringe filter. The filtrate was transferred to a NMR tube for analysis. The conversions were controlled to be low (typically between 5 and 20%) to allow assessment of the initial rates.
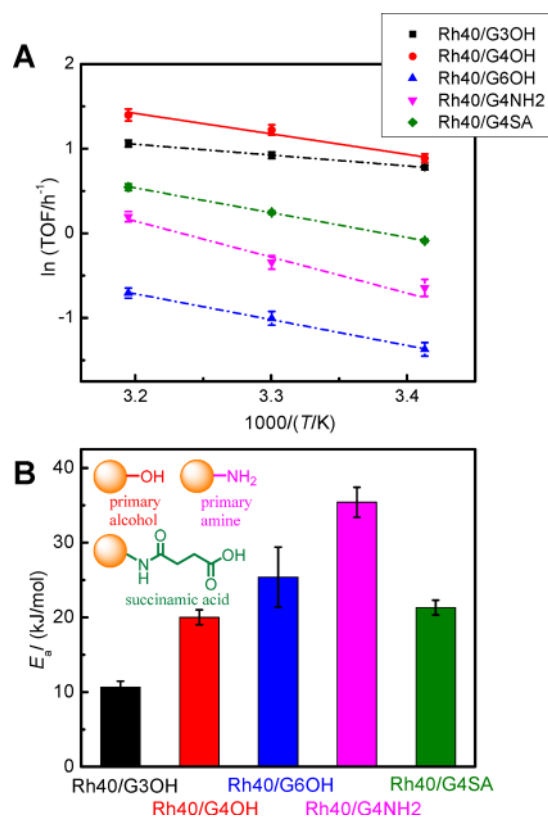


**Figure 3.** (A) Arrhenius plots of ring opening of **1** in C$_6$D$_6$ under H$_2$, catalyzed by Rh NPs with different generation number of dendrimer (G3OH, G4OH, and G6OH), and G4 dendrimer with surface groups of primary amine (G4NH$_2$) or succinamic acid (G4SA). (B) Calculated ring-opening activation energy catalyzed by the corresponding Rh NPs. Inset shows the structure of dendrimer surface groups used.

## 4. CONCLUSIONS

The ring-opening reactions of cyclopropane derivatives catalyzed by metal NPs under hydrogen were investigated. Rh$_{40}$/G4OH/SBA-15 showed a TOF of 2.24 h$^{-1}$, which was higher than the homogeneous counterparts, toward the ring opening of cyclopropylbenzene at room temperature. This catalyst was stable and could be recycled at least three times. The reaction was accelerated by electron-donating groups on the three-membered ring, while electron-accepting groups decreased the TOF. In contrast to ring-opening reactions catalyzed by homogeneous rhodium catalysts, the products of the NP catalyzed reactions were 100% linear. The apparent activation energy of the reaction was affected by the catalyst properties. For Rh NPs encapsulated in G4OH and PVP, larger particle size tends to show higher TOF and smaller reaction activation energy. For dendrimer encapsulated Rh NPs, both the dendrimer surface group and the dendrimer generation played a role in the reaction rate and activation energy of ring opening. The study sheds light on the fundamental factors controlling C−C bond activation activity and selectivity.

## ■ ASSOCIATED CONTENT

**ⓢ Supporting Information**

The Supporting Information is available free of charge on the ACS Publications website at DOI: 10.1021/jacs.6b03977.

Details of the experimental procedure and supplementary figures (PDF)

## ■ AUTHOR INFORMATION

### Corresponding Authors

*fdtoste@berkeley.edu
*somorjai@berkeley.edu

### Notes

The authors declare no competing financial interest.

## ■ ACKNOWLEDGMENTS

## ■ REFERENCES

(1) Gary, J. H.; Handwerk, G. E.; Kaiser, M. J. *Petroleum refining: technology and economics*; CRC Press: Boca Raton, FL, 2007.

(2) Beyler, C. L.; Hirschler, M. M. *SFPE handbook of fire protection engineering*; National Fire Protection Association: Quincy, MA, 2002; Vol. 2, p 110.

(3) Jun, C.-H. *Chem. Soc. Rev.* **2004**, *33*, 610.

(4) Ruhland, K. *Eur. J. Org. Chem.* **2012**, *2012*, 2683.

(5) Souillart, L.; Cramer, N. *Chem. Rev.* **2015**, *115*, 9410.

(6) Rybtchinski, B.; Milstein, D. *Angew. Chem., Int. Ed.* **1999**, *38*, 870.

(7) Bond, G. C. In *Metal-Catalysed Reactions of Hydrocarbons*; Springer: Boston, MA, 2005; p 473.

(8) Kahn, D. R.; Petersen, E. E.; Somorjai, G. A. *J. Catal.* **1974**, *34*, 294.

(9) Newham, J. *Chem. Rev.* **1963**, *63*, 123.

(10) Sridhar, T. S.; Ruthven, D. M. *J. Catal.* **1972**, *24*, 153.

(11) Capitano, A. T.; Gabelnick, A. M.; Gland, J. L. *J. Phys. Chem. B* **2000**, *104*, 3337.

(12) Gozin, M.; Weisman, A.; Ben-David, Y.; Milstein, D. *Nature* **1993**, *364*, 699.

(13) Murakami, M.; Takahashi, K.; Amii, H.; Ito, Y. *J. Am. Chem. Soc.* **1997**, *119*, 9307.

(14) Bart, S. C.; Chirik, P. J. *J. Am. Chem. Soc.* **2003**, *125*, 886.

(15) Ishida, N.; Sawano, S.; Masuda, Y.; Murakami, M. *J. Am. Chem. Soc.* **2012**, *134*, 17502.

(16) Shaw, M. H.; Melikhova, E. Y.; Kloer, D. P.; Whittingham, W. G.; Bower, J. F. *J. Am. Chem. Soc.* **2013**, *135*, 4992.

(17) Edelbach, B. L.; Vicic, D. A.; Lachicotte, R. J.; Jones, W. D. *Organometallics* **1998**, *17*, 4784.

(18) Trost, B. M.; Morris, P. J.; Sprague, S. J. *J. Am. Chem. Soc.* **2012**, *134*, 17823.

(19) Tang, C.; Jiao, N. *Angew. Chem., Int. Ed.* **2014**, *53*, 6528.

(20) Ogoshi, S.; Nagata, M.; Kurosawa, H. *J. Am. Chem. Soc.* **2006**, *128*, 5350.

(21) Dieskau, A. P.; Holzwarth, M. S.; Plietker, B. *J. Am. Chem. Soc.* **2012**, *134*, 5048.

(22) McClure, S. M.; Lundwall, M. J.; Goodman, D. W. *Proc. Natl. Acad. Sci. U. S. A.* **2011**, *108*, 931.

(23) Crooks, R. M.; Zhao, M. *Adv. Mater.* **1999**, *11*, 217.

(24) Huang, W.; Kuhn, J. N.; Tsung, C.-K.; Zhang, Y.; Habas, S. E.; Yang, P.; Somorjai, G. A. *Nano Lett.* **2008**, *8*, 2027.

(25) Witham, C. A.; Huang, W.; Tsung, C.-K.; Kuhn, J. N.; Somorjai, G. A.; Toste, F. D. *Nat. Chem.* **2010**, *2*, 36.

(26) Gross, E.; Liu, J. H.-C.; Toste, F. D.; Somorjai, G. A. *Nat. Chem.* **2012**, *4*, 947.

(27) Wilson, O. M.; Knecht, M. R.; Garcia-Martinez, J. C.; Crooks, R. M. *J. Am. Chem. Soc.* **2006**, *128*, 4510.

(28) Crespo-Quesada, M.; Yarulin, A.; Jin, M.; Xia, Y.; Kiwi-Minsker, L. *J. Am. Chem. Soc.* **2011**, *133*, 12787.

(29) Chen, W.; Ji, J.; Feng, X.; Duan, X.; Qian, G.; Li, P.; Zhou, X.; Chen, D.; Yuan, W. *J. Am. Chem. Soc.* **2014**, *136*, 16736.

(30) Ye, R.; Hurlburt, T. J.; Sabyrov, K.; Alayoglu, S.; Somorjai, G. A. *Proc. Natl. Acad. Sci. U. S. A.* **2016**, *113*, 5159.